



## Transmission dynamics of SARS-CoV-2: A modeling analysis with high-and-moderate risk populations

Salihu S. Musa<sup>a,b</sup>, Isa A. Baba<sup>c</sup>, Abdullahi Yusuf<sup>d,e,\*</sup>, Tukur A. Sulaiman<sup>d,e</sup>, Aliyu I. Aliyu<sup>e</sup>, Shi Zhao<sup>f,g</sup>, Daihai He<sup>a,\*</sup>

<sup>a</sup> Department of Applied Mathematics, Hong Kong Polytechnic University, Hong Kong

<sup>b</sup> Department of Mathematics, Kano University of Science and Technology, Wudil, Nigeria

<sup>c</sup> Department of Mathematics, Bayero University Kano, Nigeria

<sup>d</sup> Department of Computer Engineering, Biruni University, Istanbul, Turkey

<sup>e</sup> Department of Mathematics, Science Faculty, Federal University Dutse, Jigawa, Nigeria

<sup>f</sup> JC School of Public Health and Primary Care, Chinese University of Hong Kong, Hong Kong

<sup>g</sup> CUHK Shenzhen Research Institute, Shenzhen, China

### ARTICLE INFO

#### Keywords:

COVID-19

Pandemic

Reproduction number

Bifurcation

Runge–Kutta

### ABSTRACT

Nigeria is second to South Africa with the highest reported cases of COVID-19 in sub-Saharan Africa. In this paper, we employ an SEIR-based compartmental model to study and analyze the transmission dynamics of SARS-CoV-2 outbreaks in Nigeria. The model incorporates different group of populations (that is, high- and moderate risk populations) and is used to investigate the influence on each population on the overall transmission dynamics. The model, which is fitted well to the data, is qualitatively analyzed to evaluate the impacts of different schemes for control strategies. Mathematical analysis reveals that the model has two equilibria; i.e., disease-free equilibrium (DFE) which is local asymptotic stability (LAS) if the basic reproduction number ( $\mathcal{R}_0$ ) is less than 1; and unstable for  $\mathcal{R}_0 > 1$ , and an endemic equilibrium (EE) which is globally asymptotic stability (LAS) whenever  $\mathcal{R}_0 > 1$ . Furthermore, we find that the model undergoes a phenomenon of backward bifurcation (BB, a coexistence of stable DFE and stable EE even if the  $\mathcal{R}_0 < 1$ ). We employ Partial Rank Correlation coefficients (PRCCs) for sensitivity analyses to evaluate the model's parameters. Our results highlight that proper surveillance, especially movement of individuals from high risk to moderate risk population, testing, as well as imposition of other NPIs measures are vital strategies for mitigating the COVID-19 epidemic in Nigeria. Besides, in the absence of an exact solution for the proposed model, we solve the model with the well-known ODE45 numerical solver and the effective numerical schemes such as Euler (EM), Runge–Kutta of order 2 (RK-2), and Runge–Kutta of order 4 (RK-4) in order to establish approximate solutions and to show the physical features of the model. It has been shown that these numerical schemes are very effective and efficient to establish superb approximate solutions for differential equations.

### Introduction

Coronavirus disease 2019 (COVID-19) is a pandemic disease that spread very rapidly across the globe [1–5]. It has affected human lives tremendously with more than 163 million confirmed cases and killing over 3 million people in more than 220 countries and territories by May 17, 2021 [6]. As of this date, 6 January 2021, there were over 160 thousands confirmed cases including more than 2000 COVID-19 deaths cases in Nigeria [7]. COVID-19 is caused by severe acute respiratory

syndrome coronavirus 2 (SARS-CoV-2) [8] with symptoms resemble that of pneumonia, namely; dry cough, fever, and, in more severe cases, difficulty in breathing [1,9–11]. Some set of non-pharmaceutical interventions (NPIs) measures against contracting the disease were recommended by the World Health Organization (WHO) [10], they include use of face mask to cover nose and mouth, keeping a distance of at least 2 meters in public places, regular hand washing, use of tissue to cover nose when sneezing, borders and school closures, quarantine, isolation, and mass testing [10,12].

\* Corresponding authors at: Department of Applied Mathematics, Hong Kong Polytechnic University, Hong Kong (D. He). Department of Mathematics, Science Faculty, Federal University Dutse, Jigawa, Nigeria (A. Yusuf).

E-mail addresses: [yusufabdullahi@fud.edu.ng](mailto:yusufabdullahi@fud.edu.ng) (A. Yusuf), [daihai.he@polyu.edu.hk](mailto:daihai.he@polyu.edu.hk) (D. He).

<https://doi.org/10.1016/j.rinp.2021.104290>

Received 12 January 2021; Received in revised form 30 April 2021; Accepted 1 May 2021

Available online 19 May 2021

2211-3797/© 2021 The Author(s).

Published by Elsevier B.V. This is an open access article under the CC BY-NC-ND license

(<http://creativecommons.org/licenses/by-nc-nd/4.0/>).

Mathematical modeling is a very versatile and effective instrument for studying infectious disease transmission dynamics [13]. Mathematical analysis and numerical simulations of the model can be used to develop and test efficient control strategies. The predominant model of epidemiological forecast applicable to COVID-19 is based on the use of deterministic SEIR-type model which is vital in modeling aggregate population evolution under a scenario where population can be subdivided into mutually exclusive compartments [12]. See, Fig. 1 for the proposed model diagram.

Nigeria is one of the developing sub-Saharan African countries hit by the double burdens of diseases (mostly infectious) [7], whose health care system does not provide basic and regular health services adequately for its citizens even before the current pandemic of the COVID-19 [14–17]. With the emergence of COVID-19, the situation becomes even more devastating and resulted in a more serious health and socioeconomic problems [14]. However, to tackle the pandemic scenario, the Nigerian government has adopted most of the NPIs measures even before the index case detected in February 27, 2020 [7,18,14,19]. Considering the exponential increasing nature in the number of COVID-19 cases and deaths, the NPIs measures need to be strictly sustained and improve to effectively curtail the spread of the COVID-19 pandemic even with availability of the vaccine in the country [18,7]. Moreover, reports show that about 48.843% of the total population in Nigeria lives in the rural area, where there are less or no access to improved education and clean water supply which makes regular handwashing practice and face masks wearing an ideal, as well as lack of sufficient social media for dissemination of information that enhances awareness campaigns [19–21]. Hence, the provision of clean water and constant awareness programs is vital in curtailing the current pandemic in Nigeria and beyond. Thus, it is imperative to prioritize the fraction of the population at high risk when implementing pharmaceutical or non-pharmaceutical intervention control measures to effectively control the epidemic.

A lot of mathematical models have been developed recently to study and analyze the dynamics of COVID-19 epidemics [22,23,64–66]. Some models have adapted to the traditional ‘SEIR’-based [24–27]. Instead, several other models established a stochastic transition model for evaluating COVID-19 transmission, and also stressed the need for intervention strategies such as social distancing, quarantine, and isolation [28,29]. Since March 26, 2020, many countries and territories had passed COVID-19 travel restrictions, including border closures. Some countries put a restriction on domestic traveling except for the movement of essential materials. In most African countries, many people fail to comply with NPIs measures likely due to negligence and/or poor economic situation. Example, non-compliance of lock-down, social distancing, handwashing policy (due to insufficient water supply), face-

masks use, and travel restriction (movement from one community to the other), etc., causing more risk to COVID-19 infection [21]. This will eventually endanger the lives of many people, especially those residing in rural communities or in cities that are hosting a large number of internally displaced people (IDPs). These set of individuals are described as high-risk population due to the following reasons: (i) they live in rural areas where the illiteracy rate is high; (ii) poor economic situation; (iii) internally displaced people living in camps; (iv) have no access to potable water which make hands washing policy a practically impossible; and (v) insufficient medical resources. Whereas other sets of people, especially those residing in the urban areas, are considered as moderate risk population.

Considering the global scenario on the series of waves and different (new) strains of COVID-19, there is a need for more studies/research to timely and effectively curtail the spread of the disease. Thus, here, we proposed and analyzed an epidemic model that will be used to shed light and understanding on the transmission of SARS-CoV-2, and to access the role played by each sub-population (high and moderate risk populations) on the overall transmission of COVID-19 in Nigeria and beyond. The proposed model incorporates the effects of high and moderate risk populations [30,31] on the overall transmission dynamics to provide suggestions to public health practitioners and policymakers on the optimal control strategies to effectively control the spread of the disease. The model considered set of people living in urban communities as the moderate risk population, since they have more access to hospitals (adequate medical resources compared to the rural communities that are regarded as high-risk population), sufficient social media for awareness campaigns, and better transport systems, the influence of human behavior on the spread of infectious diseases, etc., which can help greatly in the prevention and control of diseases [19,32–38].

In this work, we developed an SEIR-based model to investigate the dynamics of COVID-19 in Nigeria with the effect of high-and-moderate risk populations. A noteworthy characteristic of the current model is the inclusion of the role of high-and moderate risk populations on the spread of COVID-19 infection. The model, which fitted well to the COVID-19 cases data collected from the Nigerian Center for Disease Control (NCDC) [7], is adopted to examine the impacts of different schemes for control and mitigation strategies. We examine the dynamics of the model with human-to-human transmission route and ignore other modes of transmission since most of COVID-19 infection occurs via person to person transmission route.

### Model formulation

We proposed a deterministic model based on the standard SEIR-

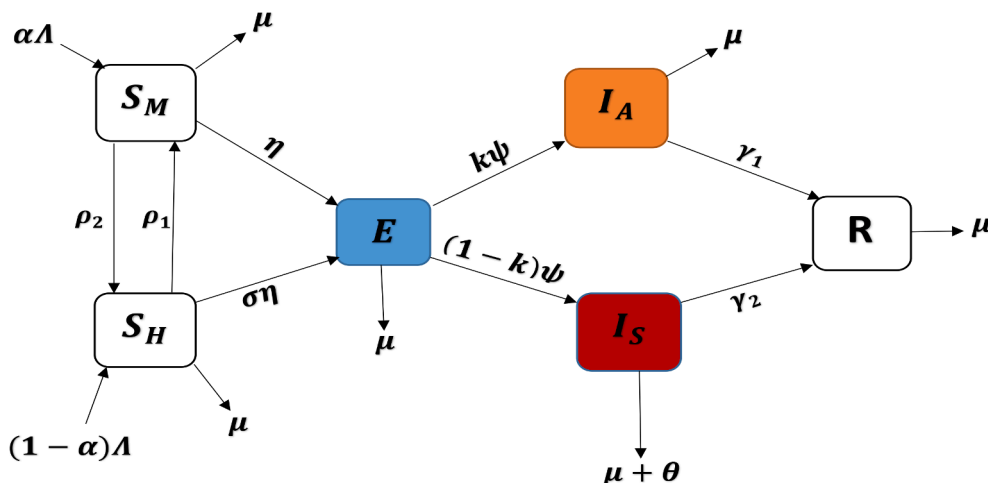


Fig. 1. The schematic diagram of the COVID-19 model with-high-and-moderate risk populations.

based model to study the transmission dynamics of the COVID-19 epidemic [30,31]. The proposed model incorporates high-and-moderate risk population to investigate the dynamics of COVID-19 transmission epidemic in Nigeria and beyond [30,31,39].

Some fraction of the population are considered to be at moderate risk due to the availability of resources such as hospitals, good transport systems, adequate social media for dissemination of information and other awareness campaigns, influences of human behavior on the spread of infectious diseases due to high rate of educated people, which helps largely in the prevention and control on the spread of infectious diseases [32,34,36–38]. The rest of the population (especially those residing in the rural areas) are regarded as high risk population due to poor resources, awareness, education, and social media.

The total human population  $N$  at time  $t$ , denoted by  $N(t)$ , is subdivided into mutually exclusive compartments, which are susceptible humans with moderate risk of COVID-19 infection ( $S_M(t)$ ), susceptible humans with high risk of COVID-19 infection ( $S_H(t)$ ), exposed humans  $e(t)$ , asymptotically infected humans  $I_A(t)$ , symptomatically infected humans ( $I_S(t)$ ), and recovered humans  $r(t)$ . Thus,  $N(t)$ , is given by  $N(t) = S_M(t) + S_H(t) + E(t) + I_A(t) + I_S(t) + R(t)$ . The model's flow diagram is depicted in Fig. 1, while the state variables and parameters (assumed to be all positive) are summarized in Table 1. The proposed model's system is given by the following non-linear ordinary differential equations

$$\begin{aligned} \frac{dS_M}{dt} &= \alpha\Lambda + \rho_1 S_H - \rho_2 S_M - \eta S_M - \mu S_M, \\ \frac{dS_H}{dt} &= (1 - \alpha)\Lambda + \rho_2 S_M - \sigma\eta S_H - \rho_1 S_H - \mu S_H, \\ \frac{dE}{dt} &= \eta(S_M + \sigma S_H) - (\psi + \mu)E, \\ \frac{dI_A}{dt} &= k\psi E - (\gamma_1 + \mu)I_A, \\ \frac{dI_S}{dt} &= (1 - k)\psi E - (\theta + \gamma_2 + \mu)I_S, \\ \frac{dR}{dt} &= \gamma_1 I_A + \gamma_2 I_S - \mu R. \end{aligned} \tag{1}$$

The force of infection of the model (1) above is given by  $\eta = \frac{\beta(\phi I_A + I_S)}{N}$ .

**Table 1**  
Interpretation of the state variables and parameters used for the Eqn (1).

Variable	Description
$N$	Total population of human
$S_M$	Susceptible humans with moderate risk of COVID-19 infection
$S_H$	Susceptible humans with high risk of COVID-19 infection
$E$	Exposed humans
$I_A$	Asymptotically infected humans
$I_S$	Symptomatically infected humans
$R$	Recovered humans
Parameter	
$\Lambda$	Recruitment rate of humans
$\alpha$	Fraction of newly recruited humans moving to $S_M$
$\sigma$	Modification parameter for the increase of infectivity of $S_H$
$\rho_1$	Rate of movement from $S_H$ to $S_M$
$\rho_2$	Rate of movement from $S_M$ to $S_H$
$\beta$	Transmission/contact rate
$\phi$	Relative infectiousness factor for asymptomatic humans
$\psi$	Disease progression rate
$k$	Fraction of infected humans moving to $I_S$
$\gamma_1$	Recovery rates from $I_1$
$\gamma_2$	Recovery rates from $I_2$
$\theta$	COVID-19 induced death rate
$\mu$	Natural death rate

In the model (1), the susceptible individuals are recruited into the population by birth (or immigration) at a rate  $\Lambda$ . A parameter  $\alpha$  represent a fraction of recruits joining the compartment,  $S_c$ , and the remaining fraction,  $1 - \rho$ , joins  $S_H$ .  $\rho_1$  and  $\rho_2$  represent movement from  $S_H$  to  $S_M$  and vice versa. Susceptible humans in  $S_M$  and  $S_H$  joins the exposed class,  $E$ , following effective contacts with an infected individual from  $I_A$  or  $I_S$ , at a rate  $\eta$  and  $\sigma\eta$ , respectively. It is worth noting that  $\sigma(\geq 1)$  account for the modification parameter for the increase of infectivity of a high-risk population. This further indicates that there will be more contact (and a high rate of non-compliance of NPIs measures) in the high-risk population than the moderate-risk population, likely due to lack of awareness, insufficient availability of resources, human behaviors, and other factors mentioned above [30,34,37,38,40].  $\psi$  denote progression rate from the exposed humans to infectious humans. A fraction  $k$  is the modification parameter that account for the reduction in infectiousness from  $E$  to  $I_A$  (and the remaining fraction,  $1 - k$ , represent modification parameter moving from  $E$  to  $I_S$ ).  $\gamma_1$  ( $\gamma_2$ ) measure the recovery rate of humans from  $I_A$  ( $I_S$ ).  $\theta$  account for the COVID-19 induced death rate, while  $\mu$  represent the natural death rate of humans.

*Basic qualitative properties of the model*

In this subsection, we qualitatively analyzed some basic property of the model (1). For mathematical convenience, the following equation represent the rate of change of the total population of humans, which is given by  $N'(t)$ . Here, the prime denotes differentiation with respect to time, and thus, following [41], we have

$$\frac{dN}{dt} = \Lambda - \theta I_S - \mu N \leq \Lambda - \mu N. \tag{2}$$

Consider solutions of Eq. (1), which is given by  $\Omega = \left\{ (S_M, S_H, E, I_A, I_S, R) \in \mathbb{R}_+^6 : N \leq \frac{\Lambda}{\mu} \right\}$ , and simplifying  $N$  it from Eqn. (2), one can see that all solutions of the model starting in  $\Omega$  remain in  $\Omega$  for all  $t \geq 0$ . Thus,  $\Omega$  is positive-invariant, and it is enough to evaluate solutions that are restricted in  $\Omega$ . Therefore, for the model (1), the existence, uniqueness and continuation results hold provided the solutions that are restricted in  $\Omega$  hold [42].

**Theoretical analysis of the model**

*Disease-free equilibrium and reproduction number*

In the absence of the disease, the infected components of the model are considered as zero (that is,  $E = I_A = I_S = R = 0$ ). Then, the DFE of the system (1), which is always feasible, obtained at steady state is given by

$$\begin{aligned} E_1^0 &= (S_M^0, S_H^0, E^0, I_A^0, I_S^0, R^0) \\ &= \left( \frac{\Lambda(\alpha\mu + \rho_1)}{\mu(\mu + \rho_1 + \rho_2)}, \frac{\Lambda((1 - \alpha)\mu + \rho_2)}{\mu(\mu + \rho_1 + \rho_2)}, 0, 0, 0, 0 \right). \end{aligned}$$

The next-generation matrix method (NGM) [43] is applied to scrutinize the characteristics of the asymptotic stability of the DFE. Specifically, adopting the expression in [43], the associated NGMs,  $F$  and  $V$ , for the new infection terms and the transition terms, are given, respectively, by

$$F = \begin{bmatrix} 0 & g_1 & g_2 \\ 0 & 0 & 0 \\ 0 & 0 & 0 \end{bmatrix} \text{ and } V = \begin{bmatrix} L_3 & 0 & 0 \\ -k\psi & L_4 & 0 \\ -(1 - k)\psi & 0 & L_5 \end{bmatrix}, \tag{3}$$

where,  $N^0 = \frac{\Lambda}{\mu}$ ,  $g_1 = \frac{\beta\phi\mu(S_M^0 + \sigma S_H^0)}{\Lambda}$ ,  $g_2 = \frac{\beta\mu(S_M^0 + \sigma S_H^0)}{\Lambda}$ ,  $b_1 = 1 - \alpha$ ,  $b_2 = 1 - k$ ,  $L_1 = \mu + \rho_2$ ,  $L_2 = \mu + \rho_1$ ,  $L_3 = \mu + \psi$ ,  $L_4 = \mu + \gamma_1$ ,  $L_5 = \mu + \gamma_2 + \theta$ . Therefore, the basic reproduction number,  $\mathcal{R}_0$ , is given by

$$\begin{aligned} \mathcal{R}_0 &= \mathcal{R}_0^A + \mathcal{R}_0^S = \frac{\psi k g_1}{L_3 L_4} + \frac{\psi(1-k)g_2}{L_3 L_5} \\ &= \frac{(((1-\alpha)\sigma + \alpha)\mu + \sigma\rho_2 + \rho_1)\beta((1-k)L_4 + kL_5\phi)\mu\psi}{(\mu + \rho_1 + \rho_2)L_3 L_4 L_5}. \end{aligned} \tag{4}$$

The threshold quantity,  $\mathcal{R}_0$ , is the basic reproduction number of the model (1), which measures the average number of secondary infections produced by a typical infected person introduced into a fully susceptible population during the period of the individual infection. It is the sum of the component reproduction numbers linked with new cases produced by asymptotically-infected ( $\mathcal{R}_0^A$ ) and symptomatically-infected ( $\mathcal{R}_0^S$ ) individuals.

For the local asymptotic stability (LAS) of the DFE of the model (1), we obtained the following result which is inline with Theorem 1 of [43].

**Theorem 1.** *The DFE,  $E_1^0$ , of the model (1), is LAS inside the region of attraction,  $\Omega$ , if  $\mathcal{R}_0 < 1$ , and unstable if  $\mathcal{R}_0 > 1$ .*

The epidemiological consequence of the above result is that a small influx of COVID-19 cases will not generate an outbreaks if  $\mathcal{R}_0 < 1$ . It should be mentioned, however, that, for epidemic models such as Eq. (1), the requirement for obtaining  $\mathcal{R}_0 < 1$  is only adequate, but not necessary, for mitigating the outbreaks. This is in addition to the fact that, in one hand, for some epidemic models the disease always dies out with time (regardless of the value of  $\mathcal{R}_0$ ). On the other hand some endemic models, the disease will persist in the community whenever  $\mathcal{R}_0 > 1$ . The reason for this is that, by allowing for the recruitment of susceptible individuals, the population of wholly-susceptible individuals is continually being replenished, thereby allowing the disease to find potential targets to infect. This allows the outbreaks to sustain itself in a population [44].

**Endemic equilibrium**

*Existence of endemic equilibria*

The endemic equilibrium, EE, of the system (1) is the steady state where the disease spreads and persists in a community, that is, when at least one of the infected compartments of the model (1) is non-empty. Suppose  $\Xi^* = (S_M^*, S_H^*, E^*, I_A^*, I_S^*, R^*)$  be an EE solution of the system (1). Equating the right hand side of the model (1) to zero, the EE in terms of  $E^*$  and  $\eta^*$ , is given by

$$\begin{aligned} S_M^* &= \frac{\Lambda(\alpha\eta^*\sigma + \alpha\mu + \rho_1)}{\eta^{*2}\sigma + ((\sigma + 1)\mu + \sigma\rho_2 + \rho_1)\eta^* + \mu(\mu + \rho_1 + \rho_2)}, \\ S_H^* &= \frac{\Lambda((\eta^* + \mu)(1-\alpha) + \rho_2)}{\eta^{*2}\sigma + ((\sigma + 1)\mu + \sigma\rho_2 + \rho_1)\eta^* + \mu(\mu + \rho_1 + \rho_2)}, \\ I_A^* &= \frac{k\psi E^*}{L_4}, \\ I_S^* &= \frac{(1-k)\psi E^*}{L_5}, \\ R^* &= \frac{E\psi(kL_5\gamma_1 + L_4(1-k)\gamma_2)}{\mu L_5 L_4}. \end{aligned} \tag{5}$$

Where the force of infection in terms of the EE is now given by

$$\eta^* = \frac{\beta(\phi I_A^* + I_S^*)}{N^*}. \tag{6}$$

Similarly, the total human population in terms of EE is given by

$$N^* = S_M^* + S_H^* + E^* + I_A^* + I_S^* + R^*. \tag{7}$$

Hence, Eq. (6) can now be written as

$$S_M^* + S_H^* + E^* + (1 - \frac{\beta\phi}{\eta^*})I_A^* + (1 - \frac{\beta}{\eta^*})I_S^* + R^* = 0. \tag{8}$$

*Existence of backward bifurcation*

In this subsection, we analyse the scenario of backward bifurcation (BB), which has been studied in previous works [45–47]. The appearance of BB in the current model indicates that  $\mathcal{R}_0 < 1$ , is although adequate, but not necessary for effectual control of the COVID-19 epidemic. Therefore, we explore the analysis of BB for the system (1) below.

Substituting Eq. (5) into Eq. (6), and solving, we have the following Eqn in terms of  $\eta^*$ ,

$$A_1\eta^{*2} + A_2\eta^* + A_3 = 0, \tag{9}$$

where,

$$\begin{aligned} A_1 &= \sigma((kL_5 + L_4(1-k))\psi + L_4L_5)\mu + \psi\sigma(kL_5\gamma_1 + L_4(1-k)\gamma_2), \\ A_2 &= (\sigma(1-\alpha) + \alpha)((kL_5 + L_4(1-k))\psi + L_4L_5)\mu^2 \\ &\quad + (((\rho_2 + \gamma_2 - \beta)(1-\alpha) + \alpha(\rho_2 - \beta))\sigma + (1-\alpha)\rho_1 + \alpha(\rho_1 + \gamma_2))(1-k)L_4 \\ &\quad + L_5k((-\beta\phi + \gamma_1 + \rho_2)(1-\alpha) + \alpha(-\beta\phi + \rho_2))\sigma + (1-\alpha)\rho_1 + \alpha(\rho_1 + \gamma_1))\psi \\ &\quad + L_5L_4(((1-\alpha)\rho_2 + \alpha(L_3 + \rho_2))\sigma + (L_3 + \rho_1)(1-\alpha) + \alpha\rho_1)\mu \\ &\quad + \psi(\sigma\rho_2 + \rho_1)(kL_5\gamma_1 + L_4(1-k)\gamma_2), \\ A_3 &= \mu(L_3L_4L_5(\rho_1 + \rho_2 + \mu) - ((\sigma(1-\alpha) + \alpha)\mu + \sigma\rho_2 + \rho_1)(k\phi L_5 + L_4(1-k))\psi\beta) \\ &= \mu L_3L_4L_5(\rho_1 + \rho_2 + \mu)[1 - \mathcal{R}_0]. \end{aligned}$$

Hence, we have the following Result 2.

**Theorem 2.** *The model system (1) has*

- i) a unique EE, if  $A_3 < 0$ ;
- ii) a unique EE, if  $A_2 < 0$  and  $A_3 = 0$ ;
- iii) two EEs, if  $A_2 < 0, A_3 > 0$  and  $\Delta > 0$ ; and
- iv) no EE otherwise.

Obviously, one can verify that, case (i) of Theorem 2 highlights the existence of unique EE of the model (1) whenever  $\mathcal{R}_0 < 1$ . While, case (iii) indicates the possibility of the existence of BB. The existence of the BB phenomenon in the current model show that the DFE which is LAS co-exists with a stable EE whenever  $\mathcal{R}_0 < 1$  [45,46,48]. To show this, the discriminant of the quadratic equation is set to zero, i.e.,  $A_2^2 - 4A_1A_3 = 0$ , then we solve for the critical value of the basic reproduction number, represented by  $\mathcal{R}_0^c$  and is given by

$$\mathcal{R}_0^c = 1 - \frac{A_2^2}{4A_1\mu L_3L_4L_5(\rho_1 + \rho_2 + \mu)}. \tag{10}$$

Hence, the following result is established.

**Lemma 3.** *The BB phenomenon exists for the Eqn (1) when case (iii) of the Theorem 2 is satisfied with  $\mathcal{R}_0^c < \mathcal{R}_0 < 1$ .*

By implications, the existence the phenomenon of BB in the model (1) divulge that the classical requirement of getting  $\mathcal{R}_0 < 1$  is although necessary but not a prerequisite for effectual control of COVID-19 epidemic. Thus, disease elimination would depend on the initial sizes of sub-populations of the model (1) [42,45,46,48–50].

*Non-existence of backward bifurcation*

In order to rule out the existence of BB for the model (1) completely, the following corollary is considered (under a special scenario where  $\sigma = 0$ ).

**Corollary 4.** *The model (1) does not undergoes BB phenomena if  $\sigma = 0$ .*

In this scenario, we set the parameter  $\sigma = 0$ , which represent modification parameter for the increase of infectiousness of  $S_H$  from the model (1), and all other parameter values remains fixed as in the Table 2. So that, the  $\mathcal{R}_0$  can now be written as  $\mathcal{R}_0^* = \frac{\beta\phi\mu S_M^0}{\Lambda} \left( \frac{\psi k}{L_3L_4} + \frac{\psi(1-k)}{L_3L_5} \right) < 1$ . Therefore, the model (1) assumes a unique stable DFE and is consistent with Theorem 1. Since, the DFE is LAS whenever  $\mathcal{R}_0^* < 1$  (see Theorem 1). Thus, the coefficients of the Eqn (7)

**Table 2**  
Baseline values of the parameters used for the model (1).

Parameter	Baseline values (day <sup>-1</sup> )	Sources
$\Lambda$	2500 (1000–5000)	[55]
$\alpha$	0.5 (0–1)	estimated by [56]
$\sigma$	1.3 (1–2)	estimated by [30]
$\rho_1$	0.0714 (0.01–0.5)	assumed
$\rho_2$	0.0461 (0.01–0.5)	assumed
$\beta$	0.745 (0.599–1.68)	[57,58]
$\phi$	0.5 (0.4–0.6)	[59]
$\psi$	0.143 (0.05–0.275)	[2,60]
$k$	0.86834 (0–1)	[60]
$\gamma_1$	1/7 (1/14–1/3)	[60]
$\gamma_2$	1/7 (1/30–1/3)	[59,60]
$\theta$	0.015 (0.001–0.1)	[58,59]
$\mu$	0.00005 (0.00003–0.00006)	[55]

are now given by

$$A_1 = 0, A_2 = \alpha((kL_5 + L_4(1 - k))\psi + L_4L_5)\mu^2 + (((1 - \alpha)\rho_1 + \alpha(\rho_1 + \gamma_2))(1 - k)L_4L_5k((1 - \alpha)\rho_1 + \alpha(\rho_1 + \gamma_1)))\psi + L_5L_4((L_3 + \rho_1)(1 - \alpha) + \alpha\rho_1)\mu + \psi\rho_1(kL_5\gamma_1 + L_4(1 - k)\gamma_2), \text{ and}$$

$$A_3 = \mu^2\pi\theta g_1g_2(1 - \mathcal{R}_0^n).$$

Therefore, according to Theorem 2, the EE does not exist when  $\mathcal{R}_0^* \leq 1$ , since the Eqns (9) will be automatically linear, i.e.,  $\eta^* = \frac{-A_3}{A_2}$ , highlighting the non-existence of EE for the model (1) whenever  $\mathcal{R}_0^* \leq 1$ . From the above, we reveal that the parameter  $\sigma$  is the cause for the existence of BB of the model (1), and obviously this parameter differentiates the compartment of high and moderate risk susceptible populations. This further revealed the role of high-and-moderate risk populations in curtailing the spread of the COVID-19 pandemic in Nigeria and beyond.

Furthermore, based on the result in Theorem 3.2, the model (1) does not undergo the phenomenon of BB at  $R_0 = 1$ . For more general discussion on BB and its causes, see [45,46,48–50]. Thus, the following global asymptotic stability result is obtained to completely rule out the existence of the BB phenomenon in the current model).

#### Global stability analysis of the endemic equilibrium

Following previous studies [45,50,51], we obtained the following result (see Theorem 5).

**Theorem 5.** *The EE of the COVID-19 model (1),  $\Xi^*$ , is globally-asymptotically stable (GAS) in the region of attraction whenever  $\mathcal{R}_0 > 1$ ,*

$$\text{with } \left(1 - \frac{\eta}{\eta^*}\right)\left(1 - \frac{I_A\eta}{I_A^*\eta^*}\right) \geq 0, \text{ and } \left(1 - \frac{\eta}{\eta^*}\right)\left(1 - \frac{I_S\eta}{I_S^*\eta^*}\right) \geq 0.$$

For the proof of the above theorem, see Appendix part.

## Simulation results

### Model fitting

The data-fitting process in this section involves implementing the Pearson’s Chi-square and the least square sampling method using the R statistical software (version 3.4.1 or above) [41]. We fitted the model (1) to the weakly COVID-19 reported cases in Nigeria from February 28 to August 13, 2020. The time series of COVID-19 reported cases for Nigeria can be obtained from the World Health Organization (WHO) available from <https://covid19.who.int/> [6] or Nigeria Center for Disease Control (NCDC) available from <https://covid19.ncdc.gov.ng/> [7]. Demographic time series and parameters were computed based on the data from the World Bank [52]. All other parameters can be found in the Table 2 and the following initial conditions:  $S_M = 10.5 \times 10^7, S_H = 8.5 \times 10^7, E =$

$12.1 \times 10^4, I_A = 12, I_S = 6$  and  $R = 2$ , with  $\theta = 0.85015(0.001 - 0.89)$ . Fig. 2 indicates the fitting results of the Eqn (1) for each of the daily and cumulative number of COVID-19 cases for Nigeria. This further shows that the proposed model can capture well the epidemics curves from the daily cases of COVID-19 for Nigeria from 28 February to 25 August.

### Sensitivity analysis

In this subsection, by adopting previous works [42,53–55], we computed Partial Rank Correlation Coefficients (PRCCs) for sensitivity analysis of the model (1). The PRCCs of the  $\mathcal{R}_0$  and infection attack rate for the sensitivity analysis of the model (1), depicted in Fig. 3, was used to reveal the influences of the model parameters on reproduction number,  $\mathcal{R}_0$ , and infection attack rate. We applied 5000 random samples taken from uniform distributions of each model parameters (see Table 2 using the R statistical software (version 3.4.1 or above) with package “sensitivity” to estimate the impact of each parameter on  $\mathcal{R}_0$  and attack rate to show the most important parameter for effectual control. Furthermore, for each random parameter sample set, the model (1) was simulated to examine the target epidemiological parameter values. We found that the most sensitive epidemic parameters of the model (1) that should be emphasized for COVID-19 control are the  $\rho_1$  and  $\rho_2$  (those parameters are directly linked to the high risk and moderate risk populations or compartments) followed by  $\beta$  and  $\gamma_2$ . This further indicates that to effectively control the COVID-19 epidemic there is a need for total (or high rate) of compliance for the NPIs measures as well as implementing movement restriction, especially from high risk to moderate risk populations and vice versa.

### Numerical simulations

Here, we use 3 efficient approaches namely EM, RK-2, and RK-4 to examine the transmission dynamics (in each scenario) of COVID-19 in Nigeria with the effect of a high-and-moderate risk population. We make a comparison with the ode45 function for each of the 3 approaches mentioned.

In the absence of an exact solution for the proposed model, we need to establish approximate solutions to show the behavior of the model (1). To this aim, the above-described numerical schemes have been employed to describe the clear vision of the behaviour of the proposed model. The initial conditions and the initial values of the parameters that have been used in carrying out the numerical results are as described in Table 2. Based on the performed numerical simulation, 4 displays the approximate outlook of the proposed model with the ODE45 function and EM.

Fig. 5 displays the approximate outlook of the proposed model with ODE45 and the RK-2 approach. It should be noted that the method of RK’s-2 provides a better approximation than EM. In this case, this is because of the indistinguishable existence of the solution.

Fig. 6 displays the approximate outlook of the proposed model with ODE45 and the RK-4 approach. The results of the RK-4 approach gave a good outcome. The overall comparison of all schemes used for the approximation of the proposed model is shown in Fig. 7. Besides, Rk-2 and Rk-4 require two and four evaluations per step and their global truncation errors are  $O(h^2)$  and  $O(h^4)$ , respectively and it is very well-known that these truncation errors measure the amount at a stated step, where the exact solutions to the differential equations fail to hold for the difference equation under consideration for approximation. This may seem like an improper way of measuring the error of multifarious methods since we want to know how well the approximations provided by the methods follow the differential equation and not the other way around. However, the exact solution is not known, so this can not generally be determined, and the truncation error can very well serve to determine not only the error of a method but also the actual approximation error.

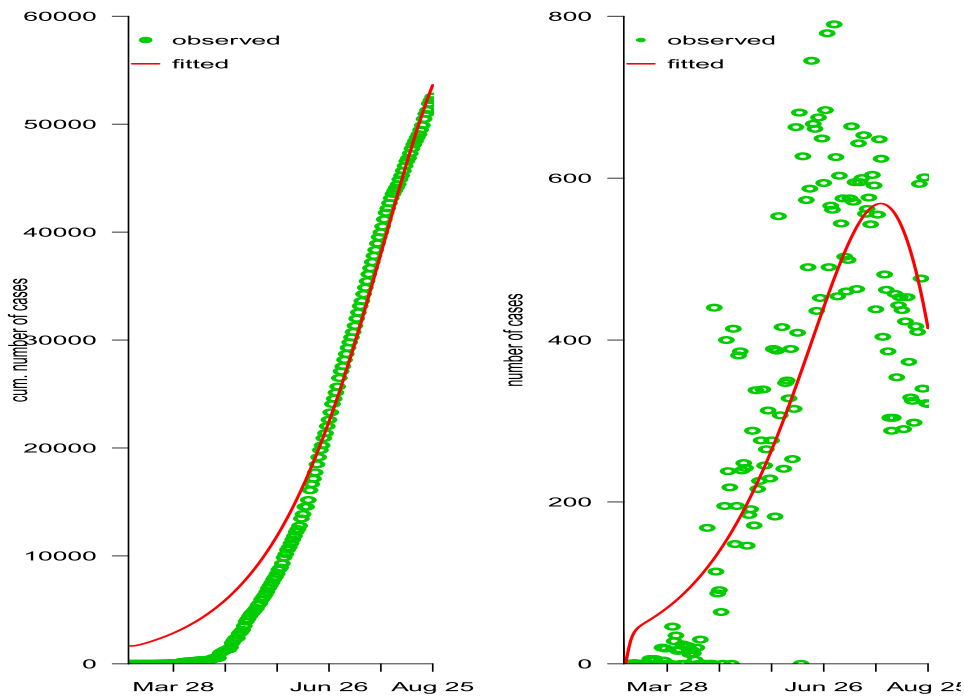


Fig. 2. Fitting results of the model (1) to the reported number of COVID-19 cases in Nigeria from February 28 to August 25, 2020. In both panels, the green dots are the observed number of cases, and the red curves are the fitting results. The left panel shows the cumulative number of cases, and the right panel represents the daily number of new cases.

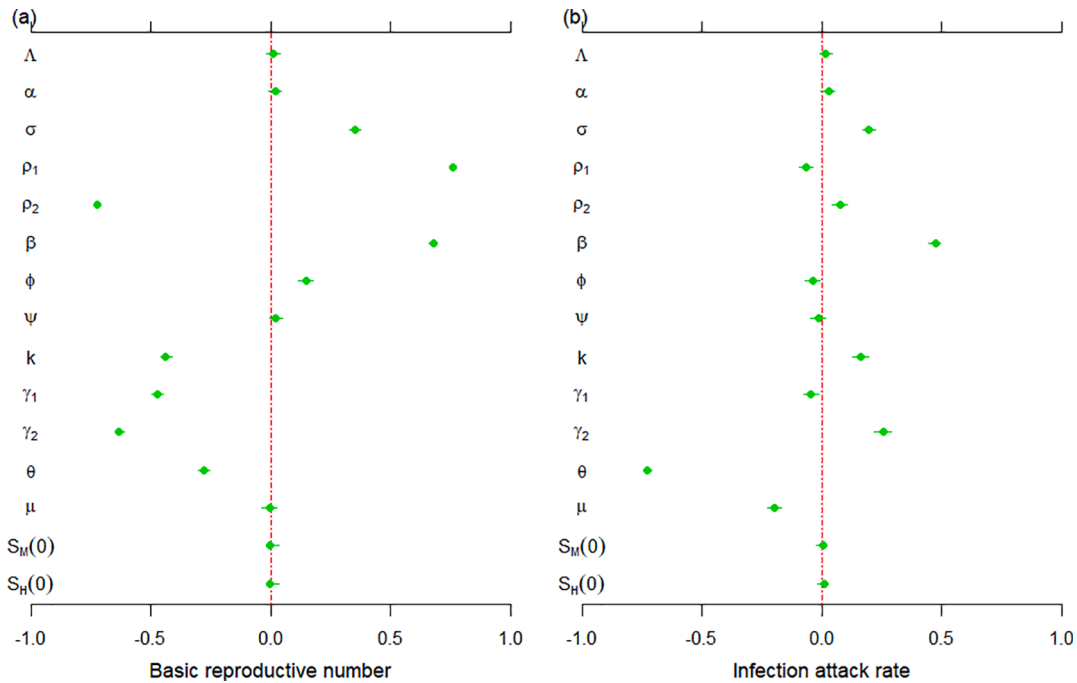


Fig. 3. Result of the Partial Ranked Correlation coefficients (PRCCs) for the basic reproduction number and infection attack rate against the model's parameters. The dots denotes the PRCCs estimates; and the bars represents the 95% confidence intervals (CI). The values and ranges of the model parameters are summarized in Table 2.

**Conclusions**

The world has been confronting an overwhelming scenario of COVID-19 pandemic caused by SARS-CoV-2, which appeared in Wuhan, China in early 2020. Despite tremendous efforts from the public health, the disease has killed over 3 million people and caused a huge burden in

the socio-economic sector globally. Although a number of vaccines are currently available (or being developed) [61], however, most of the control efforts are directed primarily on the use of non-pharmaceutical interventions (NPIs) measures, such as social-distancing, use of mask, lockdown, contact tracing, quarantine, and isolation.

In this study, we used the classical (Susceptible-Exposed-Infected-

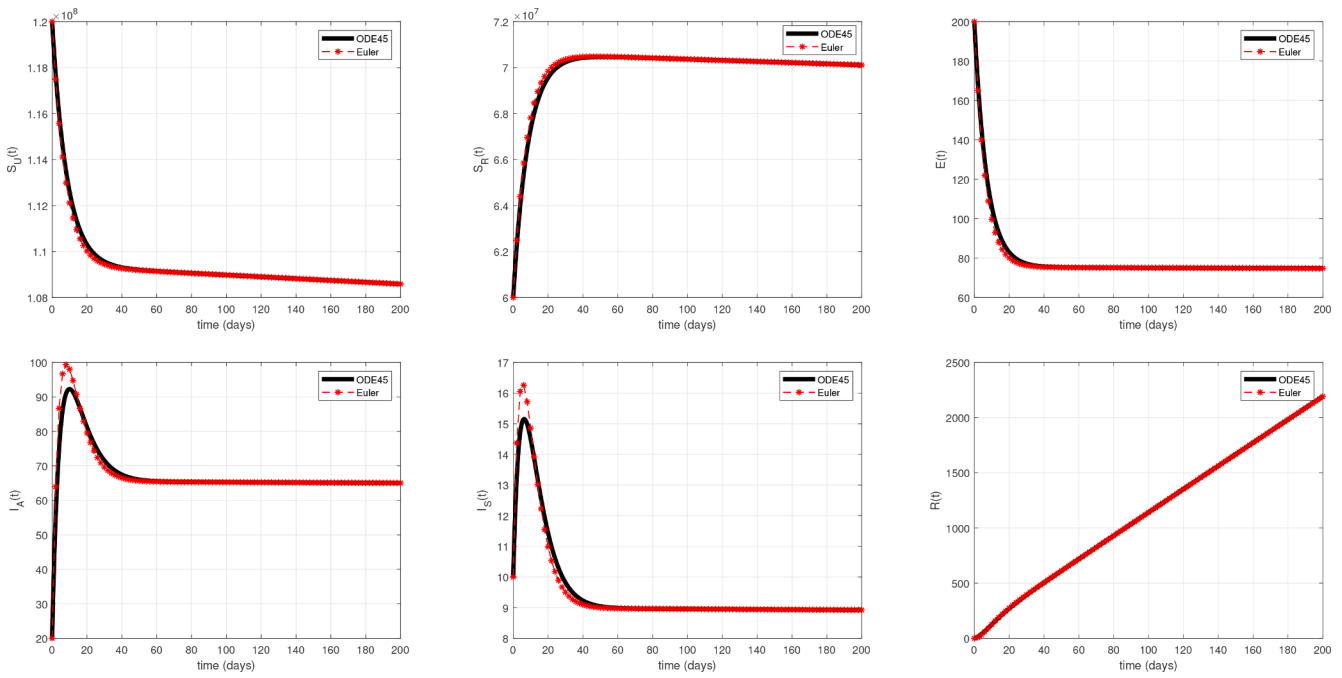


Fig. 4. EM versus ODE45 function.

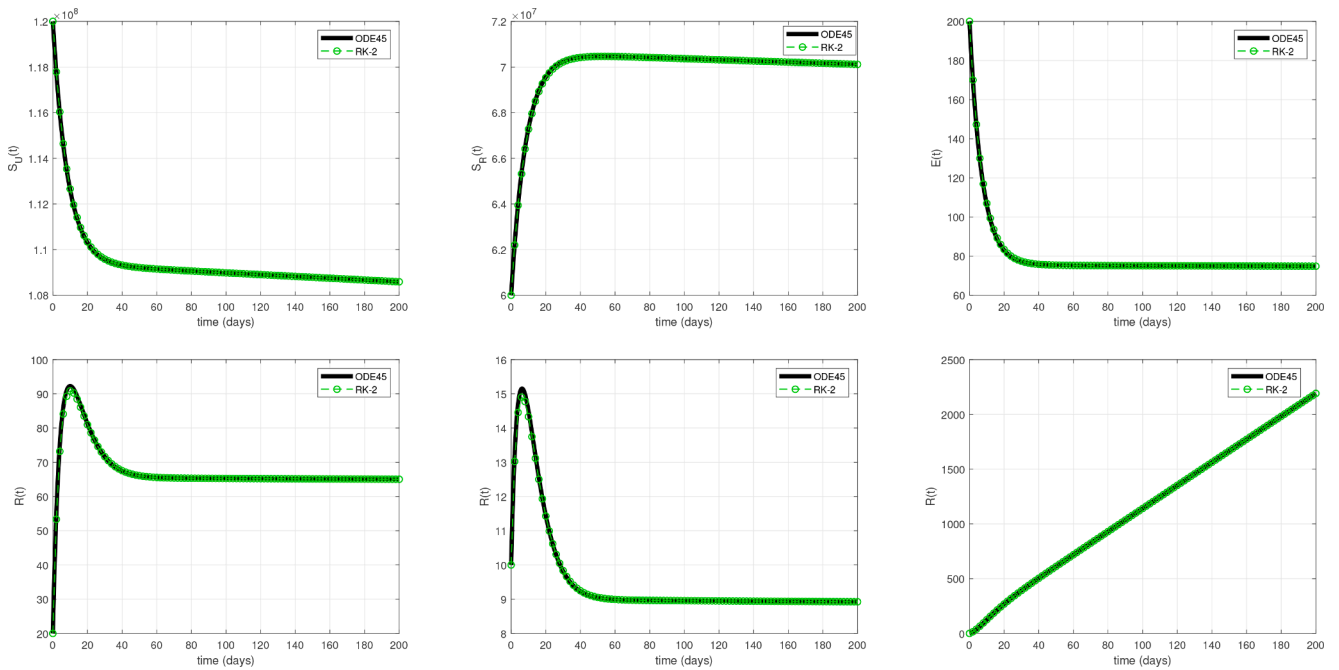


Fig. 5. RK-2 versus ODE45 function.

Recovered) SEIR-based model to qualitatively analyzed the dynamics behavior of COVID-19 infection in Nigeria with effects of high-and-moderate risk population. We computed the basic reproduction number,  $\mathcal{R}_0$ , of the proposed COVID-19 model, which was used to determined the asymptotic stability behavior of the model. Further mathematical analysis reveals that the model has two equilibria; that is, the DFE (absence of disease in a population); and the EE (speediness and persistence ability of disease in a population). The local asymptotic stability (LAS) of the DFE exists for the model (1) if the  $\mathcal{R}_0 < 1$ ; and unstable if  $\mathcal{R}_0 > 1$ . In addition, we found that the model (1) undergoes the BB phenomenon i.e., a situation where the stable DFE coexists with the

stable EE even if the  $\mathcal{R}_0 < 1$ . The epidemiological implication for the existence of the BB phenomenon in the proposed model is that, if  $\mathcal{R}_0 < 1$  the COVID-19 control would hinge on the initial size of individuals in each compartment, thereby making the control more difficult, indicating the needs for additional intervention strategy for effectual control. Our model, fitted to the cumulative number of reported cases, was able to capture well the epidemic curves from the daily cases of COVID-19 for Nigeria from 28 February to 25 August. The jump in the right panel of Fig. 2 indicates that the COVID-19 outbreaks in Nigeria may have been started earlier than reported, which is in line with previous estimates [16,62]. Moreover, we adopted the Partial Rank Correlation

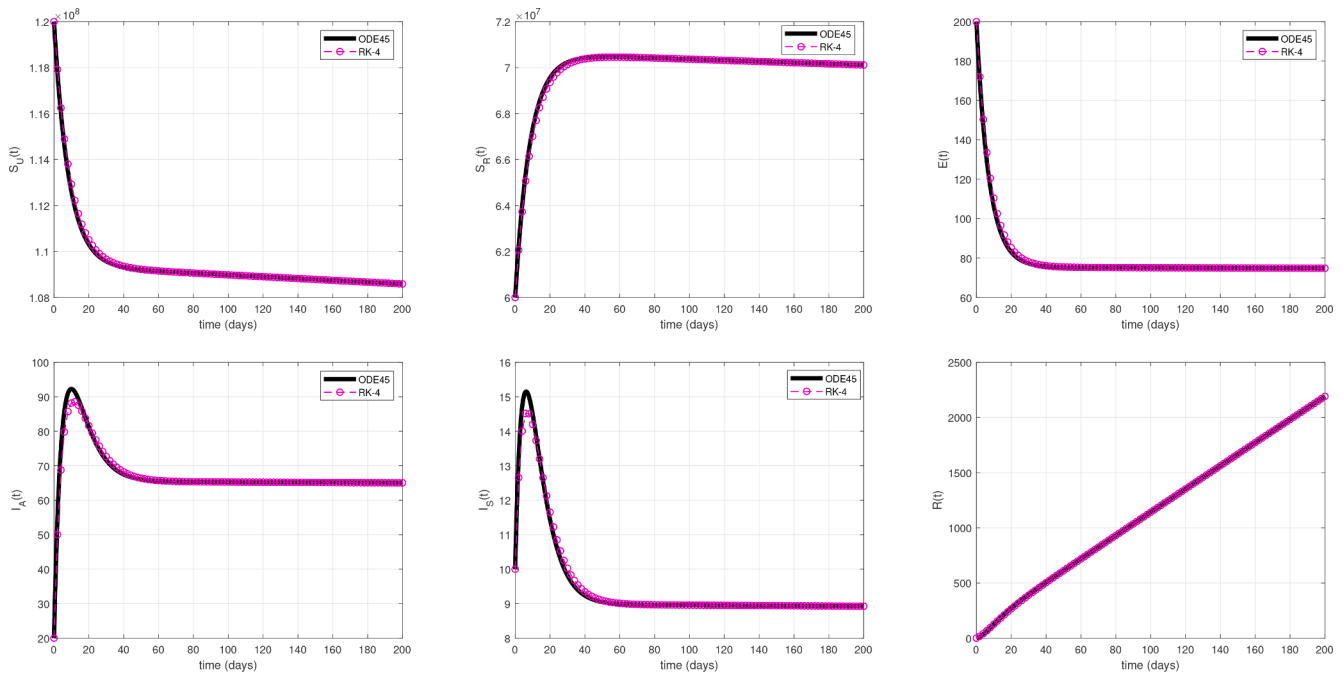


Fig. 6. RK-4 versus ODE45 function.

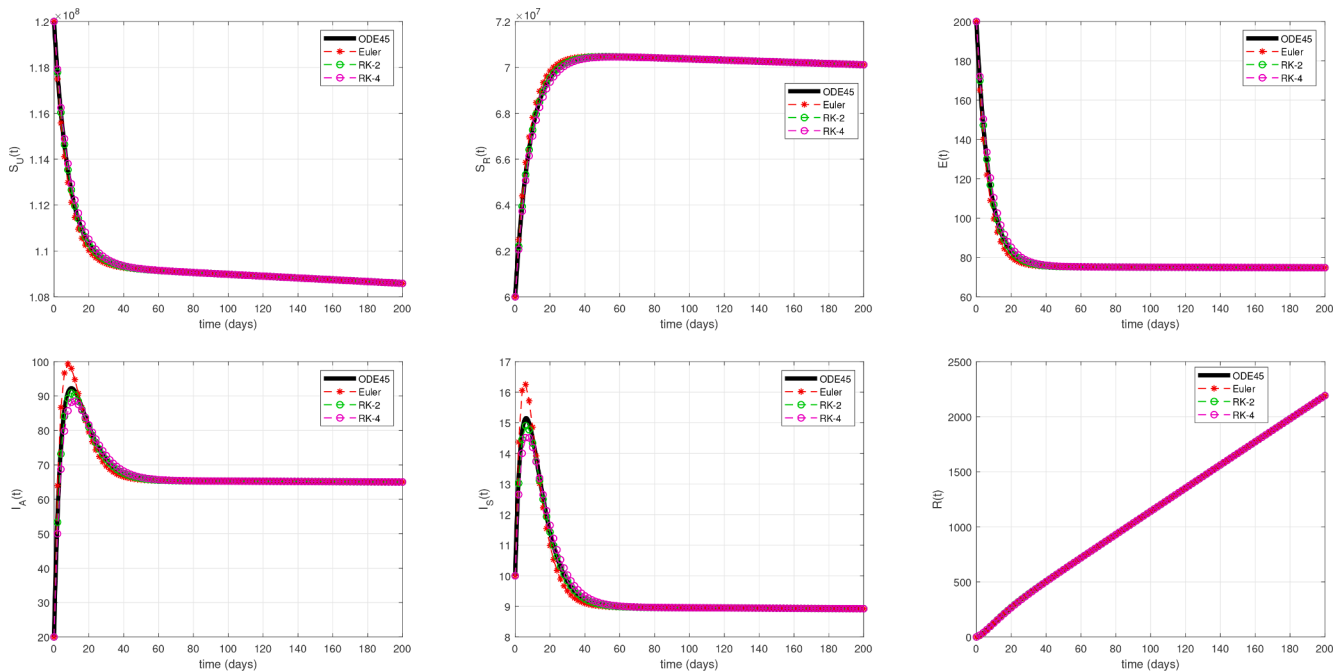


Fig. 7. Overall comparison of the 3 approaches with ODE45 function.

coefficients for the sensitivity analyses between the model outcomes and the parameters to evaluate the top rank parameters for effective control and mitigation of COVID-19 epidemic in Nigeria and beyond.

We found that the top-ranked epidemiological parameters of the model (1) that should be emphasized for controlling the COVID-19 epidemic are  $\rho_1$  and  $\rho_2$  (those parameters are directly related to the high risk and moderate risk populations or compartments), followed by transmission/contact rate ( $\beta$ ) and recovery of individuals from the symptomatically-infected compartment ( $\gamma_2$ ). Our results suggest that proper surveillance (more especially with regard to the movement of individuals from high risk to moderate risk population), testing, face-

masks use, and tracing of contacts from the suspected and confirmed cases and other NPIs measures are vital strategies and should be sustained to effectively mitigate the COVID-19 outbreaks in Nigeria.

Furthermore, since it is very difficult (nearly impossible) to obtain an exact solution for the proposed model, in this case, we designed approximate solutions to explain the approximate behavior of the model. To this end, three effective numerical schemes which are EM, RK-2, and RK-4 have been employed and compared with the well-known ODE-45 in order to explain the approximating behavior of the model. EM is one of the simplest schemes that gives a captivating approximation of the feature of each system variable.



In the literature, the singular and non-singular fractional operators have been tested to have depicted many interesting dynamics for the real-world problems. So, in the future we aim to extend the proposed model to the fractional domain in order to extract novel dynamics behaviours/features.

**Declarations**

*Ethics approval and consent to participate*

Not applicable.

*Availability of data and materials*

All materials used in this work are available in public domain.

*Funding*

DH was supported by an Alibaba (China) Co. Ltd Collaborative Research grant (ZG9Z). Other authors declared no competing interest.

*Authors' Contributions*

All authors contributed equally and gave final approval for publication of this manuscript.

**Appendix**

**Proof.** Following previous works [39,50,51], we consider the following Lyapunov function, defined by;

$$Y(t) = a_1 \left( S_M - S_M^* - S_M^* \ln \frac{S_M}{S_M^*} \right) + a_2 \left( S_H - S_H^* - S_H^* \ln \frac{S_H}{S_H^*} \right) + a_3 \left( E - E^* - E^* \ln \frac{E}{E^*} \right) + a_4 \left( I_A - I_A^* - I_A^* \ln \frac{I_A}{I_A^*} \right) + a_5 \left( I_S - I_S^* - I_S^* \ln \frac{I_S}{I_S^*} \right). \tag{A1}$$

Then, the Lyapunov derivative is given by

$$\frac{dY}{dt} = a_1 \left( 1 - \frac{S_M^*}{S_M} \right) \dot{S}_M + a_2 \left( 1 - \frac{S_H^*}{S_H} \right) \dot{S}_H + a_3 \left( 1 - \frac{E^*}{E} \right) \dot{E} + a_4 \left( 1 - \frac{I_A^*}{I_A} \right) \dot{I}_A + a_5 \left( 1 - \frac{I_S^*}{I_S} \right) \dot{I}_S.$$

Calculating terms of the above derivative, we obtain the following Eqns :

$$\begin{aligned} a_1 \left( 1 - \frac{S_M^*}{S_M} \right) \dot{S}_M &= a_1 \left( 1 - \frac{S_M^*}{S_M} \right) (\alpha \wedge + \rho_1 S_H - \rho_2 S_M - \eta S_M - \mu S_M) \\ &= a_1 \left( 1 - \frac{S_M^*}{S_M} \right) (\eta^* S_M^* + L_1 S_M^* - \eta S_M - L_1 S_M) \\ &= a_1 \eta^* S_M^* \left( 1 - \frac{S_M^*}{S_M} \right) \left( 1 - \frac{\eta S_M}{\eta^* S_M^*} \right) - L_1 \frac{(S_M - S_M^*)^2}{S_M} \leq a_1 \eta^* S_M^* \left( 1 - \frac{\eta S_M}{\eta^* S_M^*} - \frac{S_M^*}{S_M} + \frac{\eta}{\eta^*} \right) \text{ Similarly,} \\ a_2 \left( 1 - \frac{S_H^*}{S_H} \right) \dot{S}_H &\leq a_2 \delta \eta^* S_H^* \left( 1 - \frac{\eta S_H}{\eta^* S_H^*} - \frac{S_H^*}{S_H} + \frac{\eta}{\eta^*} \right), \\ a_3 \left( 1 - \frac{E^*}{E} \right) \dot{E} &= a_3 \eta^* S_M^* \left( \frac{\eta S_M}{\eta^* S_M^*} - \frac{E}{E^*} - \frac{\eta S_M E^*}{\eta^* S_M^* E} + 1 \right) + a_3 \delta \eta^* S_H^* \left( \frac{\eta S_H}{\eta^* S_H^*} - \frac{E}{E^*} - \frac{\eta S_H E^*}{\eta^* S_H^* E} + 1 \right), \\ a_4 \left( 1 - \frac{I_A^*}{I_A} \right) \dot{I}_A &\leq a_4 k \psi E^* \left( \frac{E}{E^*} - \frac{I_A}{I_A^*} - \frac{I_A^* E}{I_A E^*} + 1 \right), \text{ and} \\ a_5 \left( 1 - \frac{I_S^*}{I_S} \right) \dot{I}_S &\leq a_5 (1 - k) \psi E^* \left( \frac{E}{E^*} - \frac{I_S}{I_S^*} - \frac{I_S^* E}{I_S E^*} + 1 \right) \end{aligned} \tag{A2}$$

Setting  $a_1 = a_2 = a_3 = 1$ ,  $a_4 = \frac{\eta^* S_M^*}{k \psi E^*}$ , and  $a_5 = \frac{\eta^* \delta S_H^*}{(1-k) \psi E^*}$  and above Eqns, we obtain the following ;

$$\dot{Y} \leq \eta^* S_M^* \left( 2 - \frac{S_M^*}{S_M} - \frac{E}{E^*} - \frac{\eta S_M E^*}{\eta^* S_M^* E} + \frac{\eta}{\eta^*} \right) + \delta \eta^* S_H^* \left( 2 - \frac{S_H^*}{S_H} - \frac{E}{E^*} - \frac{\eta S_H E^*}{\eta^* S_H^* E} + \frac{\eta}{\eta^*} \right) + \eta^* S_M^* \left( \frac{E}{E^*} - \frac{I_A}{I_A^*} - \frac{I_A^* E}{I_A E^*} + 1 \right) + \delta \eta^* S_H^* \left( \frac{E}{E^*} - \frac{I_S}{I_S^*} - \frac{I_S^* E}{I_S E^*} + 1 \right) \tag{A3}$$

**CRedit authorship contribution statement**

**Salihu S. Musa:** Conceptualization, Formal analysis, Methodology, Writing - review & editing. **Isa A. Baba:** Conceptualization, Formal analysis, Methodology, Writing - review & editing. **Abdullahi Yusuf:** Conceptualization, Formal analysis, Methodology, Writing - review & editing. **Tukur A. Sulaiman:** Conceptualization, Investigation, Writing - review & editing. **Aliyu I. Aliyu:** Conceptualization, Investigation, Writing - review & editing. **Shi Zhao:** Conceptualization, Supervision, Writing - review & editing. **Daihai He:** Conceptualization, Supervision, Writing - review & editing.

**Declaration of Competing Interest**

DH was supported by an Alibaba (China) Co. Ltd Collaborative Research grant (ZG9Z). Other authors declared that they have no competing interests in this manuscript.

**Acknowledgements**

The authors are grateful to the handling editor and anonymous reviewers for their insightful comments which were used to strengthen the manuscript.

Now, we consider a function  $u(x) = 1-x + \ln x$ , thus, if  $x > 0$  it leads to  $u(x) \leq 0$ . And, if  $x = 1$ , then  $u(x) = 0$ . Therefore,  $x-1 \geq \ln(x)$  for any  $x > 0$  [50,51]. Empling the above Eqns, previous calculations, and the conditions from the GAS Theorem, we have

$$\begin{aligned} \left(2 - \frac{S_M}{S_M} - \frac{E}{E^*} - \frac{\eta S_M E^*}{\eta^* S_M^* E} + \frac{\eta}{\eta^*}\right) &= \left(-\left(1 - \frac{\eta}{\eta^*}\right)\left(1 - \frac{I_A \eta^*}{I_A^* \eta}\right) + 3 - \frac{S_M}{S_M} - \frac{\eta S_M E^*}{\eta^* S_M^* E} - \frac{I_A \eta^*}{I_A^* \eta} - \frac{E}{E^*} + \frac{I_A}{I_A^*}\right) \\ &\leq \left(-\left(\frac{S_M}{S_M} - 1\right) - \left(\frac{\eta S_M E^*}{\eta^* S_M^* E} - 1\right) - \left(\frac{I_A \eta^*}{I_A^* \eta} - 1\right) - \frac{E}{E^*} + \frac{I_A}{I_A^*}\right) \\ &\leq \left(-\ln\left(\frac{S_M \eta S_M E^* I_A \eta^*}{S_M \eta^* S_M^* E I_A^* \eta}\right) - \frac{E}{E^*} + \frac{I_A}{I_A^*}\right) = \left(\frac{I_A}{I_A^*} - \ln\left(\frac{I_A}{I_A^*}\right) + \ln\left(\frac{E}{E^*}\right) - \frac{E}{E^*}\right) \\ &\quad \text{Similarly,} \\ \left(2 - \frac{S_M}{S_M} - \frac{E}{E^*} - \frac{\eta S_M E^*}{\eta^* S_M^* E} + \frac{\eta}{\eta^*}\right) &\leq \left(\frac{I_S}{I_S^*} - \ln\left(\frac{I_S}{I_S^*}\right) + \ln\left(\frac{E}{E^*}\right) - \frac{E}{E^*}\right) \\ &\quad \text{Also,} \\ \frac{E}{E^*} - \frac{I_A}{I_A^*} - \frac{I_A^* E}{I_A E^*} + 1 &= \left(u\left(\frac{I_A^* E}{I_A E^*}\right) + \frac{E}{E^*} - \ln\left(\frac{E}{E^*}\right) - \frac{I_A}{I_A^*} + \ln\left(\frac{I_A}{I_A^*}\right)\right) \leq \frac{E}{E^*} - \ln\left(\frac{E}{E^*}\right) + \ln\left(\frac{I_A}{I_A^*}\right) - \frac{I_A}{I_A^*} \\ &\quad \text{and,} \\ \frac{E}{E^*} - \frac{I_S}{I_S^*} - \frac{I_S^* E}{I_S E^*} + 1 &= \left(u\left(\frac{I_S^* E}{I_S E^*}\right) + \frac{E}{E^*} - \ln\left(\frac{E}{E^*}\right) - \frac{I_S}{I_S^*} + \ln\left(\frac{I_S}{I_S^*}\right)\right) \leq \frac{E}{E^*} - \ln\left(\frac{E}{E^*}\right) + \ln\left(\frac{I_S}{I_S^*}\right) - \frac{I_S}{I_S^*} \end{aligned} \tag{A4}$$

Hence, from the above Eqs. (A1)–(A4)

$$\begin{aligned} V(t) &\leq \eta^* S_M^* \left(\left(\frac{I_A}{I_A^*} - \ln\left(\frac{I_A}{I_A^*}\right) + \ln\left(\frac{E}{E^*}\right) - \frac{E}{E^*}\right) + \right. \\ &\quad \delta \eta^* S_H^* \left(\left(\frac{I_S}{I_S^*} - \ln\left(\frac{I_S}{I_S^*}\right) + \ln\left(\frac{E}{E^*}\right) - \frac{E}{E^*}\right) + \right. \\ &\quad \left. \eta^* S_M^* \left(\frac{E}{E^*} - \ln\left(\frac{E}{E^*}\right) + \ln\left(\frac{I_A}{I_A^*}\right) - \frac{I_A}{I_A^*}\right) + \right. \\ &\quad \left. \delta \eta^* S_H^* \left(\frac{E}{E^*} - \ln\left(\frac{E}{E^*}\right) + \ln\left(\frac{I_S}{I_S^*}\right) - \frac{I_S}{I_S^*}\right) \right) \end{aligned} \tag{A5}$$

Therefore, according to LaSalle’s Invariance Principle [63], and combining Eqs. (A1)–(A5), we have  $\dot{Y} \leq 0$ . Also, the equality  $\dot{Y} = 0$  holds only if  $S_M = S_M^*$ ,  $S_H = S_H^*$ ,  $E = E^*$ ,  $I_A = I_A^*$ , and  $I_S = I_S^*$ .

Thus, the given EE is the only positive invariant set for the system, which is contained in the domain, omega.  $(\dot{V} \leq 0 (S_M^*, S_H^*, E^*, I_A^*, I_S^* \text{ and } R^*) \leq 0 \text{ and thus, the positive EE is GAS. } \square$

References

[1] Zhou F, Yu T, Du R, Fan G, Liu Y, Liu Z, et al. Clinical course and risk factors for mortality of adult inpatients with COVID-19 in Wuhan, China: a retrospective cohort study. *Lancet* 2020;395(102):1054–62. [https://doi.org/10.1016/S0140-6736\(20\)30566-3](https://doi.org/10.1016/S0140-6736(20)30566-3).

[2] Wu P, Hao X, Lau EHY, Wong JY, Leung KSM, Wu JT, et al. Real-time tentative assessment of the epidemiological characteristics of novel coronavirus infections in Wuhan, China, as at 22 January 2020. *Eurosurveillance* 2020;25(3):2000044. <https://doi.org/10.2807/1560-7917.ES.2020.25.3.2000044>.

[3] Wu JT, Leung K, Leung GM. Nowcasting and forecasting the potential domestic and international spread of the 2019-nCoV outbreak originating in Wuhan, China: a modelling study. *Lancet* 2020;395(10225):689–97. [https://doi.org/10.1016/S0140-6736\(20\)30260-9](https://doi.org/10.1016/S0140-6736(20)30260-9).

[4] Zhao S, Lin Q, Ran J, Musa SS, Yang G, Wang W, et al. Preliminary estimation of the basic reproduction number of novel coronavirus (2019-nCoV) in China, from 2019 to 2020: A data-driven analysis in the early phase of the outbreak. *Intern J Infect Dis* 2020;92:214–7. <https://doi.org/10.1016/j.ijid.2020.01.050>.

[5] Hamidreza N, Kulish VV. Complexity-Based Classification of the Coronavirus Disease (COVID-19). *Fractals* 2020;28(5):2050114. <https://doi.org/10.1142/S0218348X20501145>.

[6] World Health Organization (WHO). Coronavirus Disease (COVID-19) Dashboard 2021. URL <https://covid19.who.int/>. Assessed 7 January, 2021.

[7] Nigeria Center for Disease Control (NCDC). Coronavirus disease (COVID-19) pandemic 2021. URL <https://covid19.ncdc.gov.ng/>. Assessed 7 June, 2020.

[8] Li Q, Guan X, Wu P, Wang X, Zhou L, Tong Y, et al. Early transmission dynamics in Wuhan, China, of novel coronavirus-infected pneumonia. *New Engl J Med* 2020; 382:1199–207. <https://doi.org/10.1056/NEJMoa2001316>.

[9] Ding Q, Lu P, Fan Y, Xia Y, Liu M. The Clinical Characteristics of pneumonia patients coinfectd With 2019 novel coronavirus and influenza virus in Wuhan. *China J Med Virol* 2020;92(9):1549–55. <https://doi.org/10.1002/jmv.25781>.

[10] World Health Organization (WHO). Coronavirus disease (COVID-2019) pandemic 2021. URL <https://www.who.int/emergencies/diseases/novel-coronavirus-2019>. Assessed 7 January 2021.

[11] Hu B, Guo H, Zhou P, Shi ZL. Characteristics of SARS-CoV-2 and COVID-19. *Nat Rev Microbiol* 2021;19:141–54. <https://doi.org/10.1038/s41579-020-00459-7>.

[12] Gumel AB, Iboi EA, Ngonghala CN, Elbasha EH. A primer on using mathematics to understand COVID-19 dynamics: Modeling, analysis and simulations. *Infect Dis Model* 2020;6:148–68. <https://doi.org/10.1016/j.idm.2020.11.005>.

[13] William OK, Anderson GM. A contribution to the mathematical theory of epidemics. *Proceedings of the royal society of London. Series A, Containing papers of a mathematical and physical character* 1927;115(772):700–21.

[14] Gilbert M, Pullano G, Pinotti F, Valdano E, Poletto C, Boëlle PY, et al. Preparedness and vulnerability of African countries against importations of COVID-19: a modelling study. *Lancet* 2020;395(10227):871–7. [https://doi.org/10.1016/S0140-6736\(20\)30411-6](https://doi.org/10.1016/S0140-6736(20)30411-6).

[15] Ohia C, Bakarey AS, Ahmad T. COVID-19 and Nigeria: Putting the realities in context. *Intern J Infect Dis* 2020;95:279–81. <https://doi.org/10.1016/j.ijid.2020.04.062>.

[16] Musa SS, Zhao S, Wang MH, Habib AG, Mustapha UT, He D. Estimation of exponential growth rate and basic reproduction number of the coronavirus disease 2019 (COVID-19) in Africa. *Infect Dis Pov* 2020;9:96. <https://doi.org/10.1186/s40249-020-00718-y>.

[17] Musa SS, Zhao S, Hussaini N, Zhuang Z, Wu Y, Abdulhamid A, Wang MH, He D. Estimation of COVID-19 under-ascertainment in Kano, Nigeria during the early phase of the epidemics. *Alexandr Eng J* 2021;60(5):4547–54. <https://doi.org/10.1016/j.aej.2021.03.003>.

[18] World Health Organization (WHO). Coronavirus disease (COVID-2019) situation reports 2020. URL <https://www.who.int/emergencies/diseases/novel-coronavirus-2019/situation-reports/>. Assessed 2 August 2020.

[19] Peter OJ, Qureshi S, Yusuf A, Al-Shomrani M, Idowua AA. A new mathematical model of COVID-19 using real data from Pakistan. *Results Phy* 2021;24:104098.

[20] World Bank (WB). Rural population (% of total population) - Nigeria 2020. URL <https://data.worldbank.org/indicator/SP.RUR.TOTL.ZS?locations=NG>. Assessed 2 August, 2020.

[21] Iwuoha VC, Aniche ET. Covid-19 lockdown and physical distancing policies are elitist: towards an indigenous (Afro-centred) approach to containing the pandemic in sub-urban slums in Nigeria. *Local Envir* 2020;25(8):631–40. <https://doi.org/10.1080/13549839.2020.1801618>.

[22] Ahmed I, Modu GU, Yusuf A, Kumam P, Yusuf I. A mathematical model of Coronavirus Disease (COVID-19) containing asymptomatic and symptomatic classes. *Results in Physics* 2021;21:103776. <https://doi.org/10.1016/j.rinp.2020.103776>.

[23] Zarin R, Yusuf A. Analysis of fractional COVID-19 epidemic model under Caputo operator. *Math Meth Appl Sci* 2021. <https://doi.org/10.1002/mma.7294>.

- [24] He D, Artzy-Randrup Y, Musa SS, Stone L. The unexpected dynamics of COVID-19 in Manaus, Brazil: Herd immunity versus interventions. medRxiv 2021. <https://doi.org/10.1101/2021.02.18.21251809>.
- [25] Tang B, Bragazzi NL, Li Q, Tang S, Xiao Y, Wu J. An updated estimation of the risk of transmission of the novel coronavirus (2019-nCoV). *Infect Dis Model* 2020;5: 248–55. <https://doi.org/10.1016/j.idm.2020.02.001>.
- [26] Liu Z, Magal P, Seydi O, Webb G. Predicting the cumulative number of cases for the COVID-19 epidemic in China from early data. *Math Biosci Eng* 2020;17(4): 3040–51. <https://arxiv.org/abs/2002.12298>.
- [27] Musa SS, Wang X, Zhao S, Li S, Hussaini N, Wang W, et al. Heterogeneous Severity of COVID-19 in African Countries: A Modeling Approach. *Research square preprint* 2021. <https://doi.org/10.21203/rs.3.rs-316589/v1>.
- [28] Chen TM, Rui J, Wang QP, Zhao ZY, Cui JA, Yin LA. A mathematical model for simulating the phase-based transmissibility of a novel coronavirus, *Infect Dis Pov* 2020;9:4. <https://doi.org/10.1186/s40249-020-00640-3>.
- [29] Wang H, Wang Z, Dong Y, Chang R, Xu C, Yu X, et al. Phase-adjusted estimation of the number of coronavirus disease 2019 cases in Wuhan, China. *Cell Discov* 2020; 6:10. <https://doi.org/10.1038/s41421-020-0148-0>.
- [30] Ahmad MD, Usman M, Khan A, Imran M. Optimal control analysis of Ebola disease with control strategies of quarantine and vaccination. *Infect Dis Pov* 2016;5(1): 1–2. <https://doi.org/10.1186/s40249-016-0161-6>.
- [31] Riad MH, Sekamatte M, Ocom F, Makumbi I, Scoglio CM. Risk assessment of Ebola virus disease spreading in Uganda using a two-layer temporal network. *Sci Rep* 2019;9(1):1–7.
- [32] Yang C, Wang X, Gao D, Wang J. Impact of awareness programs on cholera dynamics: two modeling approaches. *Bulletin Math Bio* 2017;79(9):2109–2031.
- [33] Memon Z, Qureshi S, Memon BR. Mathematical analysis for a new nonlinear measles epidemiological system using real incidence data from Pakistan. *The Europ Physic J Plus* 2020;135(4):378.
- [34] Musa SS, Qureshi S, Zhao S, Yusuf A, Mustapha UT, He D. Mathematical modeling of COVID-19 epidemic with effect of awareness programs. *Infect Dis Model* 2021;6: 448–60. <https://doi.org/10.1016/j.idm.2021.01.012>.
- [35] Mustapha UT, Qureshi S, Yusuf A, Hincal E. Fractional modeling for the spread of Hookworm infection under Caputo operator. *Chaos Solit Fractals* 2020;137: 109878.
- [36] Funk S, Salathé M, Jansen VA. Modelling the influence of human behaviour on the spread of infectious diseases: a review. *J R Soc Inter* 2010;7(50):1247–56.
- [37] He D, Wang X, Gao D, Wang J. Modeling the 2016–2017 Yemen cholera outbreak with the impact of limited medical resources. *J Theoret Bio* 2018;451:80–5.
- [38] Baba IA, Yusuf A, Nisar KS, Abdel-Aty AH, Nofal TA. Mathematical model to assess the imposition of lockdown during COVID-19 pandemic. *Res Phys* 2021;20: 103716.
- [39] Lin Q, Musa SS, Zhao S, He D. Modeling the 2014–2015 Ebola Virus Disease Outbreaks in Sierra Leone, Guinea, and Liberia with Effect of High-and Low-risk Susceptible Individuals. *Bulletin Math Bio* 2020;82(8):1–23.
- [40] Atangana E, Atangana A. Facemasks simple but powerful weapons to protect against COVID-19 spread: Can they have sides effects? *Results Phy* 2020;103425.
- [41] Hussaini N, Okuneye K, Gumel AB. Mathematical analysis of a model for zoonotic visceral leishmaniasis. *Infect Dis Model* 2017;2(4):455–74. <https://doi.org/10.1016/j.idm.2017.12.002>.
- [42] Musa SS, Zhao S, Chan HS, Jin Z, He D. A mathematical model to study the 2014–2015 large-scale dengue epidemics in Kaohsiung and Tainan cities in Taiwan, China. *Math Biosci Eng* 2019;16:3841–63. <https://doi.org/10.3934/mbe.2019190>.
- [43] Van den Driessche P, Watmough J. Reproduction numbers and sub-threshold endemic equilibria for compartmental models of disease transmission. *Math Biosci* 2002;180:29–48. [https://doi.org/10.1016/S0025-5564\(02\)00108-6](https://doi.org/10.1016/S0025-5564(02)00108-6).
- [44] Van den Driessche P. Reproduction numbers of infectious disease models. *Infect Dis Model* 2017;2(3):288–303. <https://doi.org/10.1016/j.idm.2017.06.002>.
- [45] Garba SM, Gumel AB, Bakar MA. Backward bifurcations in dengue transmission dynamics. *Math Biosci* 2008;215(1):11–25. <https://doi.org/10.1016/j.mbs.2008.05.002>.
- [46] Gumel AB. Causes of backward bifurcations in some epidemiological models. *J Math Anal Appl* 2012;395:355–65. <https://doi.org/10.1016/j.jmaa.2012.04.077>.
- [47] Yang C, Wang X, Gao D, Wang J. Impact of awareness programs on cholera dynamics: two modeling approaches. *Bull Math Biol* 2017;79(9):2109–31. <https://doi.org/10.1007/s11538-017-0322-1>.
- [48] Musa SS, Hussaini N, Zhao S, He D. Dynamical analysis of chikungunya and dengue co-infection model. *Disc Cont Dyn Sys -B* 2020;25(5):1907–33. <https://doi.org/10.3934/dcdsb.2020009>.
- [49] Agosto FB. Mathematical model of Ebola transmission dynamics with relapse and reinfection. *Math Biosci* 2017;283:48–59. <https://doi.org/10.1016/j.mbs.2016.11.002>.
- [50] Roop-O P, Chinviriyasit W, Chinviriyasit S. The effect of incidence function in backward bifurcation for malaria model with temporary immunity. *Math Biosci* 2015;265:47–64. <https://doi.org/10.1016/j.mbs.2015.04.008>.
- [51] Sun G, Xie J, Huang S, Jin Z, Li M, Liu L. Transmission dynamics of cholera: Mathematical modeling and control strategies. *Commun Nonlinear Sci Numer Simulat* 2017;45:235–44. <https://doi.org/10.1016/j.cnsns.2016.10.007>.
- [52] World Bank (WB). Data, Population 2020. URL <https://data.worldbank.org/indicator/SP.POP.TOTL?locations=NG>. Accessed December 2020.
- [53] Gao D, Lou Y, He D, Porco TC, Kuang Y, Chowell G, Ruan S. Prevention and control of Zika as a mosquito-borne and sexually transmitted disease: a mathematical modeling analysis. *Sci Rep* 2016;6(1):28070. <https://doi.org/10.1038/srep28070>.
- [54] Zhao S, Stone L, Gao D, He D. Modelling the large-scale yellow fever outbreak in Luanda, Angola, and the impact of vaccination. *PLoS Negl Trop Dis* 2018;12(1): e0006158. <https://doi.org/10.1371/journal.pntd.0006158>.
- [55] Musa SS, Zhao S, Gao D, Lin Q, Chowell G, He D. Mechanistic modelling of the large-scale Lassa fever epidemics in Nigeria from 2016 to 2019. *J Theoret Bio* 2020;493:110209. <https://doi.org/10.1016/j.jtbi.2020.110209>.
- [56] Musa SS, Zhao S, Hussaini N, Habib AG, He D. Mathematical modeling and analysis of meningococcal meningitis transmission dynamics. *Intl J Biomath* 2020;13(1): 2050006. <https://doi.org/10.1142/S1793524520500060>.
- [57] Lin Q, Zhao S, Gao D, Lou Y, Yang S, Musa SS, et al. A conceptual model for the outbreak of Coronavirus disease 2019 (COVID-19) in Wuhan, China with individual reaction and governmental action. *Intl J Infect Dis* 2020;93:211–6. <https://doi.org/10.1016/j.ijid.2020.02.058>.
- [58] Musa SS, Gao D, Zhao S, Yang L, Lou Y, He D. Mechanistic modeling of the coronavirus disease 2019 (COVID-19) outbreak in the early phase in Wuhan, China, with different quarantine measures. *Acta Math Appl Sinica* 2020;43(2): 350–64.
- [59] Eikenberry SE, Mancuso M, Iboi E, Phan T, Eikenberry K, Kuang Y, Kostelich E, Gumel AB. To mask or not to mask: Modeling the potential for face mask use by the general public to curtail the COVID-19 pandemic. *Infect Dis Model* 2020;5: 293–308. <https://doi.org/10.1016/j.idm.2020.04.001>.
- [60] Tang B, Wang X, Li Q, Bragazzi NL, Tang S, Xiao Y, Wu J. Estimation of the transmission risk of the 2019-nCoV and its implication for public health interventions. *J Clin Med* 2020;9:462. <https://doi.org/10.3390/jcm9020462>.
- [61] World Health Organization (WHO). COVID-19 vaccines (2021). URL <https://www.who.int/emergencies/diseases/novel-coronavirus-2019/covid-19-vaccines>. Assessed 7 January 2021.
- [62] Iboi EA, Sharomi OO, Ngonghala CN, Gumel AB. Mathematical Modeling and Analysis of COVID-19 pandemic in Nigeria. medRxiv (2020). <https://doi.org/10.1101/2020.05.22.20110387>.
- [63] LaSalle JP. The stability of dynamical systems, Regional Conference Series in Applied Mathematics, SIAM Philadelphia, 1976.
- [64] Thabet ST, Abdo MS, Shah K, Abdeljawad T. Study of transmission dynamics of COVID-19 mathematical model under ABC fractional order derivative. *Results Phy* 2020;19:103507.
- [65] Fatima B, Zaman G, Alqudah MA, Abdeljawad T. Modeling the pandemic trend of 2019 Coronavirus with optimal control analysis. *Results Phy* 2021;20:103660.
- [66] Ali A, Khan MY, Sinan M, Allehiany FM, Mahmoud EE, Abdel-Aty AH, Ali G. Theoretical and numerical analysis of novel COVID-19 via fractional order mathematical model. *Results Phy* 2021;20:103676.